



HAL
open science

What controls precipitation delta O-18 in the southern Tibetan Plateau at seasonal and intra-seasonal scales? A case study at Lhasa and Nyalam

Jing Gao, Valérie Masson-Delmotte, Camille Risi, You He, Tandong Yao

► To cite this version:

Jing Gao, Valérie Masson-Delmotte, Camille Risi, You He, Tandong Yao. What controls precipitation delta O-18 in the southern Tibetan Plateau at seasonal and intra-seasonal scales? A case study at Lhasa and Nyalam. *Tellus B - Chemical and Physical Meteorology*, 2013, 65 (1), pp.21043. 10.3402/tellusb.v65i0.21043 . hal-01108537

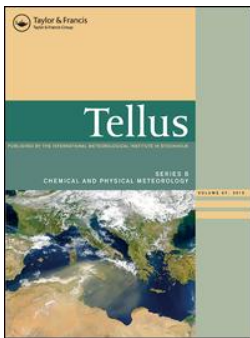
HAL Id: hal-01108537

<https://hal.science/hal-01108537>

Submitted on 29 Oct 2020

HAL is a multi-disciplinary open access archive for the deposit and dissemination of scientific research documents, whether they are published or not. The documents may come from teaching and research institutions in France or abroad, or from public or private research centers.

L'archive ouverte pluridisciplinaire **HAL**, est destinée au dépôt et à la diffusion de documents scientifiques de niveau recherche, publiés ou non, émanant des établissements d'enseignement et de recherche français ou étrangers, des laboratoires publics ou privés.



What controls precipitation $\delta^{18}\text{O}$ in the southern Tibetan Plateau at seasonal and intra-seasonal scales? A case study at Lhasa and Nyalam

Jing Gao, Valerie Masson-Delmotte, Camille Risi, You He & Tandong Yao

To cite this article: Jing Gao, Valerie Masson-Delmotte, Camille Risi, You He & Tandong Yao (2013) What controls precipitation $\delta^{18}\text{O}$ in the southern Tibetan Plateau at seasonal and intra-seasonal scales? A case study at Lhasa and Nyalam, *Tellus B: Chemical and Physical Meteorology*, 65:1, 21043, DOI: [10.3402/tellusb.v65i0.21043](https://doi.org/10.3402/tellusb.v65i0.21043)

To link to this article: <https://doi.org/10.3402/tellusb.v65i0.21043>



© 2013 J. Gao et al.



Published online: 31 Oct 2013.



Submit your article to this journal [↗](#)



Article views: 715



View related articles [↗](#)



Citing articles: 44 View citing articles [↗](#)

What controls precipitation $\delta^{18}\text{O}$ in the southern Tibetan Plateau at seasonal and intra-seasonal scales? A case study at Lhasa and Nyalam

By JING GAO^{1,4*}, VALERIE MASSON-DELMOTTE², CAMILLE RISI³, YOU HE^{1,4} and TANDONG YAO^{1,4*}, ¹Key Laboratory of Tibetan Environment Changes and Land Surface Processes, Institute of Tibetan Plateau Research, Chinese Academy of Sciences, Beijing, China; ²LSCE, UMR 8212 CEA/CNRS/UVSQ – IPSL, Gif-sur-Yvette, France; ³LMD/IPSIL, CNRS, UPMC, Paris, France; ⁴State Key Laboratory of Cryospheric Sciences, Cold and Arid Regions Environment and Engineering Research Institute, Chinese Academy Sciences, Beijing, China

(Manuscript received 4 April 2013; in final form 6 September 2013)

ABSTRACT

Understanding the spatial and temporal controls of precipitation $\delta^{18}\text{O}$ in the southern Tibetan Plateau of central Asia is necessary for paleoclimate reconstructions from the wealth of regional archives (ice cores, lake sediments, tree ring cellulose, and speleothems). While classical interpretations of such records were conducted in terms of local precipitation, simulations conducted with atmospheric general circulation models enabled with water stable isotopes have suggested that past changes in south Asia precipitation $\delta^{18}\text{O}$ may be driven by remote processes linked to moisture transport. Studies conducted at the event scale can provide constraints to assess the drivers of precipitation $\delta^{18}\text{O}$ and the validity of simulated mechanisms. Here, we take advantage of new event precipitation $\delta^{18}\text{O}$ monitored from January 2005 to December 2007 at two southern Tibetan Plateau stations (Lhasa and Nyalam). The drivers of daily to seasonal variations are investigated using statistical relationships with local and regional temperature, precipitation amount and convective activity based on in situ data and satellite products. The strongest control on precipitation $\delta^{18}\text{O}$ at Lhasa during the monsoon season at event and seasonal scales is provided by the integrated regional convective activity upstream air mass trajectories, cumulated over several days. In contrast, the integrated convection appears to be the main driver of precipitation $\delta^{18}\text{O}$ at Nyalam only in July and August, and the situation is more complex in other months. Local climate variables can only account for a small fraction of the observed $\delta^{18}\text{O}$ variance, with significant differences between both stations. This study offers a better constraint on climate archives interpretation in the southern Tibetan Plateau. The daily data presented here also provides a benchmark to evaluate the capacity of isotopically enabled atmospheric general circulation models (iGCMs) to simulate the response of precipitation $\delta^{18}\text{O}$ to convection. This is illustrated using a nudged and zoomed simulation with the LMDZiso model. While it successfully simulates some seasonal and daily characteristics of precipitation $\delta^{18}\text{O}$ in the southern Tibetan Plateau, it fails to simulate the correlation between $\delta^{18}\text{O}$ and upstream precipitation. This calls for caution when using atmospheric models to interpret precipitation $\delta^{18}\text{O}$ archives in terms of past monsoon variability.

Keywords: stable isotopes, precipitation, regional convection, southern Tibetan Plateau

1. Introduction

Records of precipitation $\delta^{18}\text{O}$ in natural archives provide key paleoclimate information in mid and low latitudes. The Tibetan Plateau (TP) encompasses the largest number of glaciers outside the polar regions (Yao et al., 2012), which

provides direct, high resolution archives of past precipitation complemented by indirect archives in speleothems, lake sediments or tree ring cellulose (e.g. Danis et al., 2006; DeCelles et al., 2007; Cai et al., 2010; Henderson et al., 2010; Griebinger et al., 2011). However, the full use of this information remains limited due to uncertainties associated with the climatic interpretation of precipitation $\delta^{18}\text{O}$ data in these regions. This is illustrated with the interpretation of South Asian speleothem $\delta^{18}\text{O}$ and lake sediment $\delta^{18}\text{O}$.

*Corresponding authors.
email: gaojing@itpcas.ac.cn; tdyao@itpcas.ac.cn

Temperature-driven distillation effects dominate the variability of temperate to polar precipitation $\delta^{18}\text{O}$, and were shown to also be the main control on northern TP precipitation $\delta^{18}\text{O}$ (Yao et al., 1996; Thompson et al., 1997; Tian et al., 2001; Wang et al., 2003; Aizen et al., 2006). The climatic drivers of southern TP $\delta^{18}\text{O}$ appear more controversial. Some studies suggested that southern TP ice core $\delta^{18}\text{O}$ reflects long-term changes in regional temperature (Thompson et al., 2000; Aizen et al., 2006; Yao et al., 2006), while others interpreted the ice core data in terms of amount effect (the anti-correlation between $\delta^{18}\text{O}$ and local precipitation amount) and Indian monsoon intensity (Vuille et al., 2005; Zhang et al., 2005; Kaspari et al., 2007; Joswiak et al., 2010). It was also suggested that the impacts of temperature or precipitation amount on southern TP $\delta^{18}\text{O}$ may not be stable through time (Tian et al., 2003; Johnson and Ingram, 2004). Based on modern spatial and seasonal relationships with local precipitation amounts, data were interpreted to reflect past changes in local monsoon intensity (e.g. Wang et al., 2005; Cai et al., 2010; An et al., 2011; An et al., 2012). Precipitation $\delta^{18}\text{O}$ is however an integrated tracer of climate and water cycle conditions, depending on phase changes affecting water vapour from evaporation to condensation. In South Asia, observations and simulations conducted with atmospheric general circulation models (AGCMs) have identified other drivers of precipitation $\delta^{18}\text{O}$ such as the variability of moisture sources, transport processes and large scale atmospheric circulation (Hoffmann and Heimann, 1997; Araguas-Araguas et al., 1998; Aggarwal et al., 2004; Ishizaki et al., 2012). Past climate simulations conducted with AGCMs equipped with water stable isotopes have shown mechanisms where changes in the large scale atmospheric circulation at the orbital scale (Legrande and Schmidt, 2009) or during abrupt glacial events (Lewis et al., 2010; Pausata

et al., 2011) do control the isotopic distillation upstream of the studied sites. However, large uncertainties remain on the ability of these models to resolve correctly the processes controlling precipitation $\delta^{18}\text{O}$, in particular convective processes (Bony et al., 2008; Lee et al., 2009; Vimeux et al., 2011).

Recent studies in South American or West African monsoon regions and northeast China have revealed the importance of local and upstream convective processes, rainout effects, droplet re-evaporation, continental recycling, and atmospheric moisture residence time governing water vapour and precipitation $\delta^{18}\text{O}$ (Bony et al., 2008; Risi et al., 2008a and 2008b; Risi et al., 2010a; Vimeux et al., 2005; Vimeux et al., 2011; Aggarwal et al., 2012; Tremoy et al., 2012; Kong et al., 2013). Such mechanisms can only be deciphered at the precipitation event scale, requiring high resolution monitoring data. Here, we aim to make use of modern observations, at the event to seasonal scale, in order to assess the processes controlling the present-day variability of precipitation $\delta^{18}\text{O}$, to better constrain climate archives interpretation and to test the realism of AGCMs. Complementing studies conducted in other monsoon regions, we focus here on the southern Tibetan Plateau, thanks to new data obtained at the event-basis. Precipitation falling in this region originates from moisture having undergone strong convection during its transport above the Indian subcontinent (Chakravarty et al., 2013; Tyrlis et al., 2013).

Here, we present and investigate 3-yr long records of precipitation $\delta^{18}\text{O}$ from two stations (Lhasa and Nyalam) in the southern TP (Fig. 1) obtained from January 2005 to December 2007, a period representative of average climatic conditions in this area. The sampling was conducted at the event-scale, allowing a focus on sub-seasonal to seasonal variations. The comparison of the two stations (at a distance of 530 km) located at similar elevations (3658 and

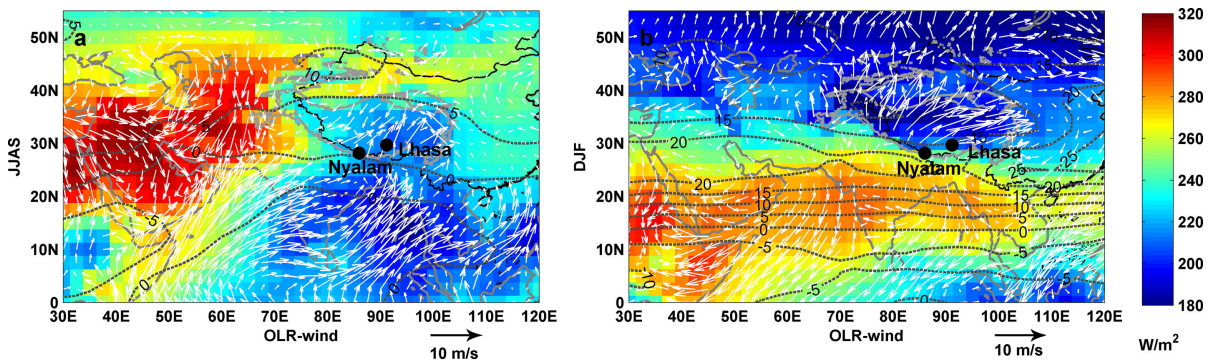


Fig. 1. 2005–2007 averaged Outgoing Long Wave radiation (OLR, shading, downloaded from http://www.esrl.noaa.gov/psd/data/gridded/data.interp_OLR.html) showing convective activity as minima in OLR due to cold cloud tops and 500 hpa zonal wind speed (dashed contours) and wind vectors (arrows, downloaded from <http://www.esrl.noaa.gov/psd/data>). The zonal wind isolines highlight the Tibetan high-pressure system. The surface wind vectors clearly depict the Indian monsoon flow and the westerlies (a) in summer (JJAS) and (b) in winter (DJF).

3810 m a.s.l., respectively) is important to assess the spatial variability associated with the drivers of precipitation $\delta^{18}\text{O}$. Because the difference of altitude between the two stations is small (~ 150 m), any altitude effect will be negligible. Lhasa is located in the valley along the Brahmaputra River (Table 1) and receives more than 80% of total annual precipitation in the monsoon season (June–September). Nyalam, located southwards of Lhasa, has colder mean conditions and its precipitation is regularly distributed year round (37% in spring, March–May, and 37% in summer, June–September). The southern TP climate is characterised by remarkable shifts in atmospheric circulation from winter, marked by the westerlies, to summer, dominated by the Indian monsoon and intense convective activity in the Bay of Bengal (BOB) and Indian subcontinent (Fig. 1).

This paper focuses on the local and regional controls of precipitation $\delta^{18}\text{O}$ in the southern TP at seasonal and intra-seasonal scales. For this purpose, we examine, based on statistical analyses: (1) the local and regional temperature/precipitation amount controls on precipitation $\delta^{18}\text{O}$; (2) the influence of local and regional convective activity on precipitation $\delta^{18}\text{O}$; (3) the influence of upstream convective activity and air mass origins on precipitation $\delta^{18}\text{O}$; (4) the ability of isotopically enabled AGCMs to resolve the controls of southern TP precipitation $\delta^{18}\text{O}$, with an illustration of a model-data comparison using one such model, LMDZiso.

2. Data

2.1. Station data

For the period 2005–2007, 294 events were collected at Lhasa, and 317 events at Nyalam with a gap at Nyalam from August to September 2005 because of missing collection (Table 1). All of the $\delta^{18}\text{O}$ measurements were conducted with respect to VSMOW at the Key Laboratory of CAS for Tibetan Environment and Land Surface Processes, China, using a MAT-253 mass spectrometer with an analytical precision of 0.05‰.

Precipitation was sampled right after the end of each event, and relevant meteorological conditions such as temperature at the beginning and the end of each precipitation event and precipitation amount were recorded. The daily (monthly, annual) precipitation $\delta^{18}\text{O}$ is the weighted mean of events $\delta^{18}\text{O}$ in the same day (month, year) as $\delta^{18}\text{O} = \sum_i^n \delta_i P_i / \sum_i^n P_i$, where $\delta^{18}\text{O}$ indicates the amount weighted $\delta^{18}\text{O}$ averages; δ_i and P_i refer to the $\delta^{18}\text{O}$ and corresponding precipitation amount of individual precipitation event; and n defines the total events occurring in one day/month/year.

2.2. Atmospheric information

To complement local meteorological data, satellite products were used to characterise regional precipitation and convective activity. Daily and monthly precipitation data from the GPCP (Global Precipitation Climatology Project) are available for our period of interest at spatial resolutions of $1^\circ \times 1^\circ$ (daily scale) and $2.5^\circ \times 2.5^\circ$ (monthly scale) (<http://www.esrl.noaa.gov/psd/data/gridded/data.gpcp.html>). Daily and monthly OLR data were also used at $2.5^\circ \times 2.5^\circ$ resolution (http://www.esrl.noaa.gov/psd/data/gridded/data.interp_OLR.html). The Outgoing Longwave Radiation (hereafter OLR) is a tracer of deep tropical convection. Low OLR values correspond to cold and high clouds identifying enhanced convection, and a negative relationship is generally shown between OLR and convection (Wang and Xu, 1997).

In addition, the moisture transport paths are identified using the HYSPLIT back trajectory model combined with NCEP reanalysis data (<ftp://arlftp.arlhq.noaa.gov/pub/archives/reanalysis/>) at 6-h time steps back to 5 d at 1000 AGL (above ground level). The clustered results are compared at Lhasa and Nyalam at the monthly scale.

2.3. Isotope-enabled general circulation modelling

The state-of-the-art LMDZiso model is used here to explore the drivers of the isotopic variations in the southern TP in a physically consistent framework. The LMDZ is the

Table 1. Summary of precipitation data at Lhasa and Nyalam stations from 2005 to 2007

Station	Latitude	Longitude	Elevation	Period	n	T (°C)	P (mm)	Annual $\delta^{18}\text{O}$ (‰)
Lhasa	29° 42' N	91° 08' E	3658 m	2005 Jan 10–2005 Oct 29	130	11.55	475	−16.36
				2006 Mar 13–2006 Nov 4	95	12.25	322.5	−13.23
				2007 Feb 5–2007 Nov 6	69	12.58	470.6	−15.59
				2005 Jan 8–2005 Dec 24	72	3.02	468.1	−10.04
Nyalam	28° 11' N	85° 58' E	3810 m	2006 Jan 31–2006 Dec 13	134	5.96	669.5	−15.06
				2007 Feb 4–2007 Sep 28	111	6.89	499	−15.22

“n” = number of samples.

Note that no samples were obtained in August and September 2005 at Nyalam.

atmospheric component of the IPSL model. Water in its vapour and condensed forms is advected by the Van Leer advection scheme (1977). Risi et al. (2010b) describe in detail the implementation of water stable isotopes in LMDZiso. It is run here with 19 vertical levels and a stretched grid characterised by 50 km resolution over southern, Eastern and Central Asia (Gao et al., 2011). Such high resolution has been shown to be necessary for a correct simulation of isotopic seasonal cycles over the TP (Gao et al., 2011).

3. Results

In this section, we use statistical analyses to assess the relationships between intra-seasonal to seasonal variations of precipitation $\delta^{18}\text{O}$ with local and regional temperature, precipitation amount and convective activity. The relationships between air mass trajectories and upstream precipitation and convective activity are then investigated.

3.1. Relationships between local climate and precipitation $\delta^{18}\text{O}$

The seasonal cycle of precipitation $\delta^{18}\text{O}$ is marked by summer depletion at Nyalam and Lhasa (Fig. 2). Annual mean $\delta^{18}\text{O}$ are 1.6‰ more depleted at Lhasa than at Nyalam. Daily

$\delta^{18}\text{O}$ variability is larger at Lhasa than at Nyalam (full range of 40.6‰ at Lhasa and 35.4‰ at Nyalam). However, summer $\delta^{18}\text{O}$ levels are about 2‰ lower at Nyalam than at Lhasa (-18.26‰ vs. -16.62‰), due to the higher $\delta^{18}\text{O}$ in June at Lhasa. Altogether, 71 summer precipitation events (JJAS) occur simultaneously at both sites. As shown in Fig. 2a and 2b, a few remarkable events are also documented, e.g. on 16 August 2005, 17 August 2007, 24 September 2007 (high precipitation amounts combined with minima in $\delta^{18}\text{O}$), 2 July 2006, and 20 July 2007 (high precipitation amounts combined with higher than -10‰ $\delta^{18}\text{O}$).

The relationships between temperature and precipitation $\delta^{18}\text{O}$ appear complex. At the seasonal scale, the data depict an inverse relationship between $\delta^{18}\text{O}$ and temperature, due to summer depletion (Fig. 2c and 2d). Significant positive correlations are observed between JJAS daily $\delta^{18}\text{O}$ and temperature, with correlation coefficients of 0.27 (Lhasa) and 0.32 (Nyalam) ($p < 0.01$). At the monthly scale, no relationship is observed between Lhasa $\delta^{18}\text{O}$ and temperature. However, at Nyalam, considering all the JJAS monthly data for the 3 yr of observation, a positive correlation exists ($n = 10$, $R = 0.67$, $p < 0.05$).

This brief analysis highlights the complex relationships between southern TP $\delta^{18}\text{O}$ and temperature. Particularly remarkable is the fact that: (1) a temperature effect is observed in the southern TP at event scale, even in summer;

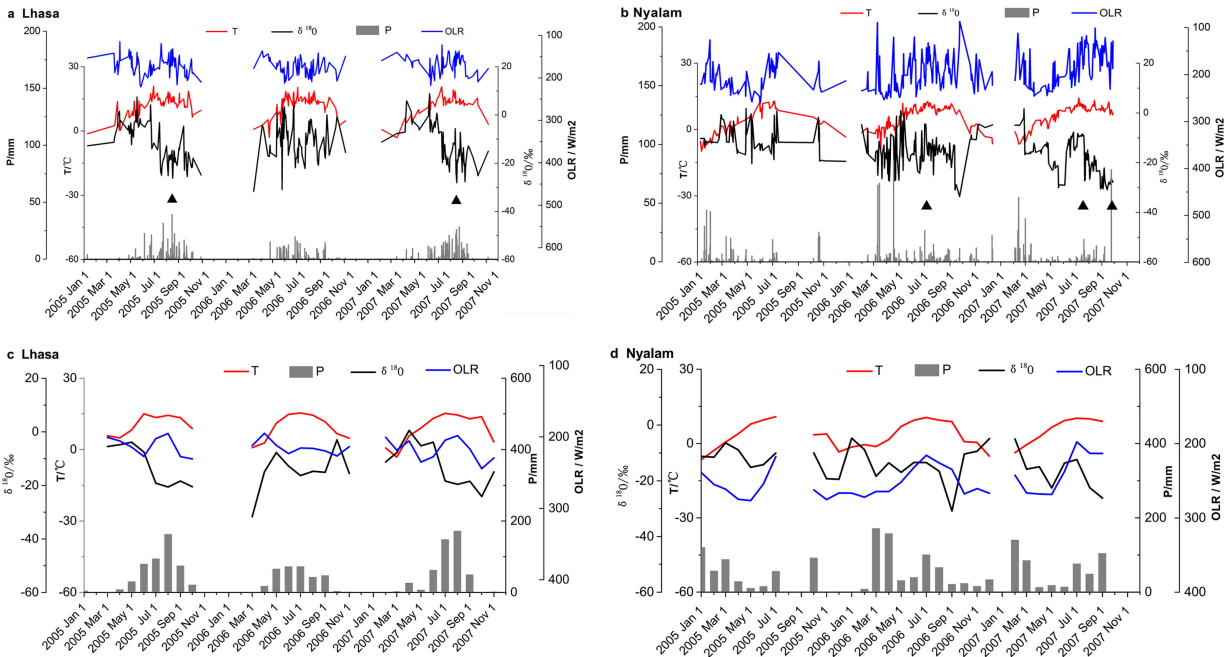


Fig. 2. Temporal variations of daily precipitation $\delta^{18}\text{O}$ and local temperature, precipitation amount and OLR at Lhasa (a) and Nyalam (b) from 2005 to 2007. Seasonal patterns of monthly weighted precipitation $\delta^{18}\text{O}$, corresponding monthly mean temperature, precipitation amount and local OLR at Lhasa (c) and Nyalam (d) during 2005–2007. The black triangles highlight extreme events (identified from peak precipitation combined with depleted $\delta^{18}\text{O}$) at both stations on 16 August 2005, 17 August 2007, 24 September 2007, 2 July 2006 and 20 July 2007.

and (2) the $\delta^{18}\text{O}$ -temperature relationship depends on the time scales and location, i.e. a temperature effect is detected at intra-seasonal and seasonal scales at Nyalam, but not at Lhasa at the seasonal scale.

Processes other than temperature therefore must also account for spatial and temporal $\delta^{18}\text{O}$ variations. While winter precipitation is related to long distance moisture transport by the westerlies, summer precipitation is related to the Indian monsoon transporting moisture from the BOB or Arabian Sea (AS). Summer precipitation (JJAS) accounts for $\sim 85\%$ of annual amounts at Lhasa, and $\sim 33\%$ at Nyalam during 2005–2007.

It has long been identified that precipitation $\delta^{18}\text{O}$ is anti-correlated with precipitation amounts (“amount effect”) in the southern TP at daily and seasonal scales (Dansgaard, 1964; Tian et al., 2001; Gao et al., 2011). At Lhasa, the daily $\delta^{18}\text{O}$ gradually decreases from May to September (Fig. 2a), showing a negative correlation with precipitation amounts ($R = -0.39$, $p < 0.01$). A similar but insignificant anti-correlation is observed in other seasons. At Nyalam, precipitation received from 2005 to 2007 is 30% larger than at Lhasa (1637 mm compared to 1268 mm). While here the amount effect is weaker and non-significant in summer, extreme precipitation events coincide with $\delta^{18}\text{O}$ minima (Fig. 2b). No amount effect is detected in other months (October–May) at the event scale at Nyalam. While the “amount effect” persists at Lhasa when considering monthly data ($R = -0.27$, $p > 0.05$), it is not detected at Nyalam, implying different controlling mechanisms.

This statistical analysis of the relationships between precipitation $\delta^{18}\text{O}$ and meteorological conditions at Lhasa and Nyalam shows that local climate variables can only account for a small fraction of the observed $\delta^{18}\text{O}$ variance (typically less than 10%), and points to significant differences of the relationships between precipitation $\delta^{18}\text{O}$ and meteorological conditions at stations within 500 km inside the southern TP.

We now explore the relationships between precipitation $\delta^{18}\text{O}$ and local convective activity, using OLR data at the corresponding $2.5^\circ \times 2.5^\circ$ grid point (“local” OLR, Fig. 2). At Lhasa, seasonal variations of $\delta^{18}\text{O}$ appear to co-vary with OLR, with highest values in May and lowest values in August. At the daily scale, a positive correlation between daily $\delta^{18}\text{O}$ and local OLR ($R = 0.48$, $p < 0.01$) is identified in JJAS, but no significant correlation can be detected in other months. We conclude that a stronger relationship is identified with convective activity than with local surface climate parameters in JJAS, at Lhasa. At Nyalam, a weaker positive correlation is found between daily $\delta^{18}\text{O}$ and OLR in JJAS ($R = 0.17$, $p < 0.05$), without significant correlation in April–May and October–March. The results from Nyalam and Lhasa depict different relationships

between $\delta^{18}\text{O}$ and OLR (local convective activity) during the pre-monsoon and monsoon seasons.

Stronger relationships between $\delta^{18}\text{O}$ and OLR emerge when individual events are aggregated into monthly averages (Fig. 2c and 2d). At Lhasa, correlation coefficients reach 0.72 ($n = 12$, $p < 0.01$) when considering monthly values during JJAS. The influence of OLR on precipitation $\delta^{18}\text{O}$ at Lhasa is stronger than at Nyalam, consistent with our earlier findings regarding local precipitation amount effect. Non-local processes may therefore control Nyalam $\delta^{18}\text{O}$ variations.

The strongest correlations with OLR than with local precipitation amounts may be due to the fact that OLR averaged in a $2.5^\circ \times 2.5^\circ$ grid box represents convection at a larger spatial scale (Risi et al., 2008b). This leads us to exploring the effect of convection at the regional scale.

3.2. Relationships between regional climate and precipitation $\delta^{18}\text{O}$

Here, the daily and monthly GPCP precipitation amounts are used to explore the influence of regional precipitation amount on precipitation $\delta^{18}\text{O}$ based on temporal correlation analyses. As shown in Fig. 3a, daily $\delta^{18}\text{O}$ at Lhasa is correlated with precipitation amount in the sectors $25^\circ\text{--}30^\circ\text{N}/75^\circ\text{--}83^\circ\text{E}$ and $26^\circ\text{--}32^\circ\text{N}/86^\circ\text{--}92^\circ\text{E}$, with correlation coefficients of $-0.16 \sim -0.27$ in JJAS ($p < 0.05$), while no significant correlation can be identified for Nyalam (Fig. 3c). The strongest negative correlation is detected with monthly precipitation amount in the sector $20^\circ\text{--}32^\circ\text{N}/80^\circ\text{--}91^\circ\text{E}$ (hereafter Zone 1, Fig. 3e, black rectangle). A remarkable positive correlation between precipitation $\delta^{18}\text{O}$ and OLR also emerges when considering daily regional OLR data (Fig. 3g and 3h). In particular, the correlation is significant in Zone 1. A stronger correlation with OLR than with precipitation was already noticed in the African monsoon region and attributed to the large scale character of OLR (Risi et al., 2008b). This suggests that Lhasa precipitation $\delta^{18}\text{O}$ is strongly related to variations in large-scale convective activity. In contrast, none of these factors can explain the variability of Nyalam precipitation $\delta^{18}\text{O}$ in JJAS (Fig. 3f and 3h). In winter, no relationship can be identified at daily or monthly scales for Lhasa or Nyalam (Fig. 3b and 3d). This is probably due to the lack of convection over North India during this season. In contrast, a slightly positive correlation is found between daily $\delta^{18}\text{O}$ at Nyalam and precipitation amount in a small south region (Fig. 3d).

So far, we have only looked at synchronous variations in convective activity and precipitation $\delta^{18}\text{O}$. Convective processes may have integrated impacts on water vapour over several J_m days preceding precipitation events. This integrative effect has been evidenced in other monsoon

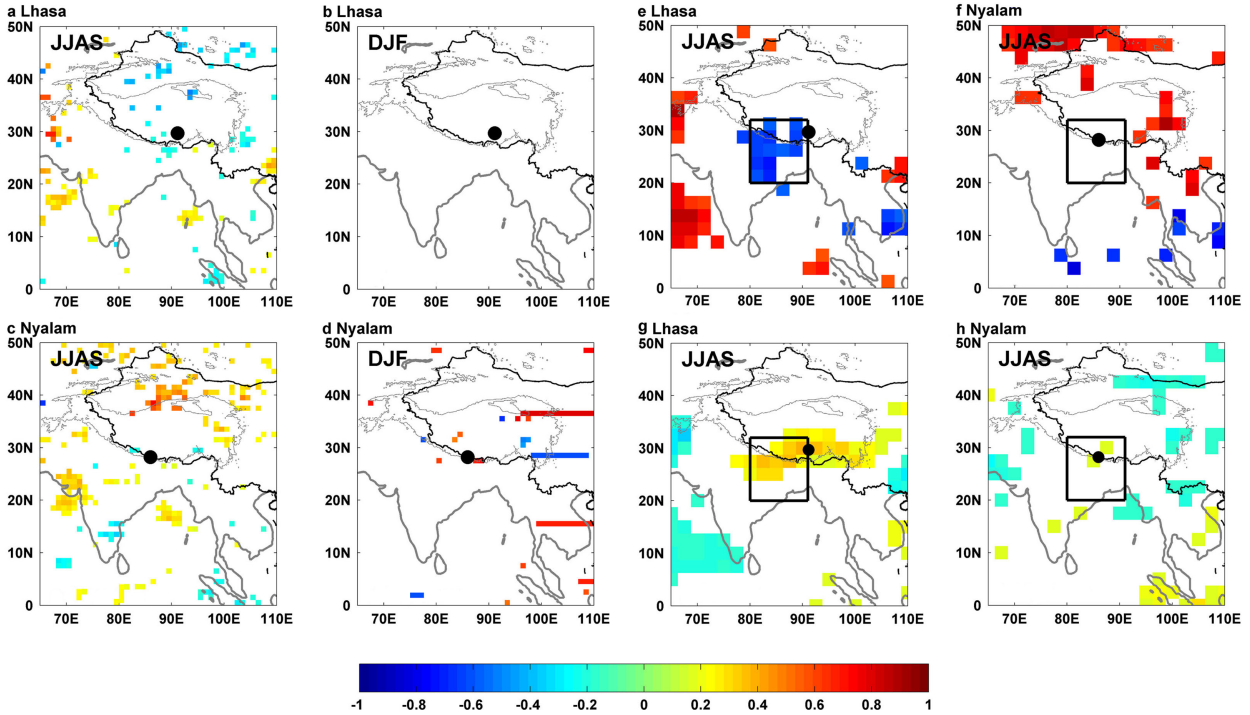


Fig. 3. Temporal correlations between daily precipitation $\delta^{18}\text{O}$ at Lhasa (a) or at Nyalam (c) and precipitation amount in other grid points of the domain, in JJAS. (b) and (d): same as (a) and (c) but for DJF. (e) and (f): same as (a) and (c) but for monthly data. Temporal correlations between daily precipitation $\delta^{18}\text{O}$ at Lhasa (g) or at Nyalam (h) and OLR in other grid points of the domain, in JJAS. On all maps, only correlations significant at the 95% confidence level are shown. The black rectangle shows the Zone 1 region discussed in the text.

regions (Risi et al., 2008b; Vimeux et al., 2011; Tremoy et al., 2012). At Lhasa, a significant correlation is found between $\delta^{18}\text{O}$ and OLR in June and July provided the latter is averaged over the 3 d (J_m) preceding the rainy events (Fig. 4a and 4e, $R=0.76$, $p<0.05$), whereas the instantaneous correlation is 0.53 ($p<0.05$). In August–September (Fig. 4a and 4i), the strongest correlation coefficient reaches 0.54 ($p<0.05$) obtained when integrating OLR over 8 d. During the whole monsoon season (JJAS), the positive correlation is remarkably strong in the southern TP and northeast India when integrating OLR over 8 d ($R \sim 0.7$, $p<0.01$, Fig. 4j), while there is no correlation found in winter (DJF) due to few events (Fig. 4k). Our analysis reveals a larger integration time before the monsoon season (April–May) and at the end of the monsoon season (September), and a minimum integration time in June–July (Fig. 4a). We suggest that this arises from the seasonal variation of the intensity and frequency of convective systems of the monsoon flow. In April and May, before the monsoon onset, the convective activity is weak and the water vapour isotopic composition integrates the signatures of convective systems during a long interval. After the monsoon onset (June and July), the convective activity is more intense, frequent, and characterised by

a large northward moisture flux. In this case, a shorter time interval is needed to erase the signature of preceding convective systems. At the end of the monsoon season, convective systems can stagnate near Lhasa, resulting in a longer moisture residence time.

At Nyalam, similar results are obtained although with longer integration times varying from 10 d in April to ~ 20 d in July–August, decreasing to 7 d in September (Fig. 4b). In July–August, a much stronger correlation between precipitation $\delta^{18}\text{O}$ and OLR is obtained with OLR integrated over 20 d ($R=0.72$, Fig. 4i) than with instantaneous OLR ($R=0.24$, $p<0.05$). In JJAS, there is also a positive correlation between precipitation $\delta^{18}\text{O}$ and OLR ($R<0.5$) in the regions surrounding Nyalam (Fig. 4m). In DJF, a conspicuous positive correlation appears in the northern BOB (Fig. 4n), which may indicate that moisture advected from BOB controls the winter precipitation at Nyalam. We attribute this longer integration period to the blocking effect of the High Himalayas on moisture transport to Nyalam area.

We also note the strong positive correlation between precipitation $\delta^{18}\text{O}$ at Lhasa (JJAS) (Fig. 4e, 4i and 4j) and Nyalam (JA and JJAS) (Fig. 4l and 4m) and OLR activity in Zone 1. This is the strongest common feature depicted

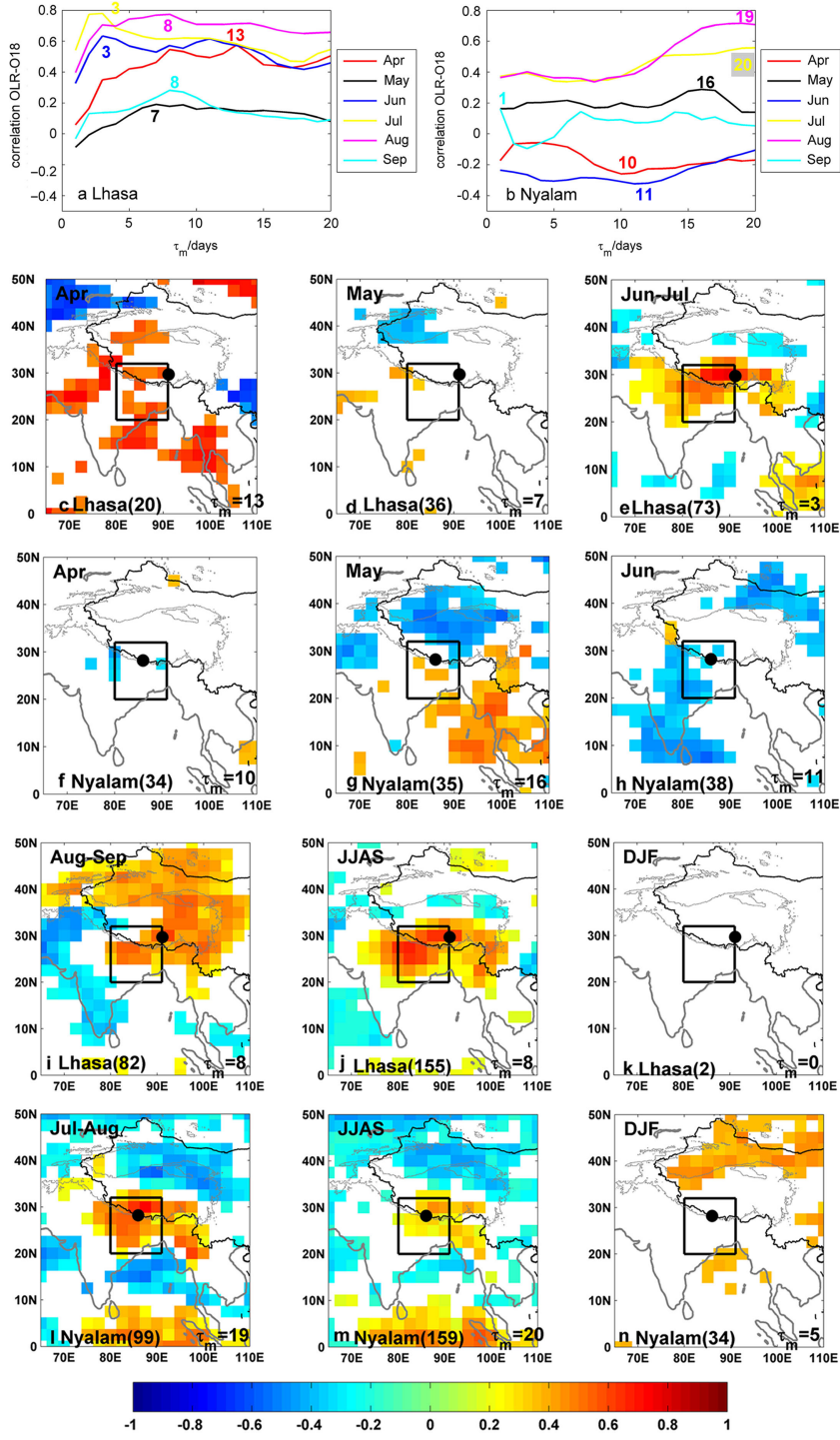


Fig. 4. Correlation coefficient (R) between the precipitation $\delta^{18}\text{O}$ and local OLR averaged over J_m days (period prior to the event over which the convective activity is averaged) at Lhasa (a) and Nyalam (b). The numbers indicate the maximum values of J_m days for each period. (c) Correlation between the $\delta^{18}\text{O}$ of events at Lhasa and the OLR averaged over the 13 d preceding each event in April, (d) 7 d preceding each event in May, (e) 3 d preceding each event in June–July, (i) 8 d preceding each event in August–September, and (j) 8 d preceding each event in JJAS. (k) No correlation can be calculated in DJF at Lhasa as only two events occurred. (f) Correlation between the $\delta^{18}\text{O}$ of events at Nyalam and the OLR averaged over the 10 d preceding each event in April, (g) 16 d preceding each event in May, (h) 11 d preceding each event in June, (l) 19 d preceding each event in July–August, (m) 20 d preceding each event in JJAS and (n) 5 d preceding each event in DJF. The numbers in brackets indicate the number of events in different months. The black rectangle shows the Zone 1 region discussed in the text.

for both Lhasa and Nyalam. This reveals that precipitation $\delta^{18}\text{O}$ in the southern TP is affected by upstream regional convection activity. The similar J_m days in September at Lhasa and Nyalam (8 and 7 d, respectively) may reflect that the integrated monsoon convective activity is the main control of precipitation $\delta^{18}\text{O}$ in September. At Lhasa, a positive correlation between daily $\delta^{18}\text{O}$ and OLR in the region of $5\text{--}20^\circ\text{N}/80\text{--}110^\circ\text{E}$ observed in April (Fig. 4c) may reflect the fact that it is affected by processes taking place during monsoon onset (Wu et al., 2012).

3.3. Air mass trajectories

We now use the HYSPLIT model to calculate air mass trajectories for Lhasa and Nyalam. Back trajectories are computed with the NCEP reanalysis data using a 6-h time

step back to 5 d at 1000 AGL. The results are then clustered at the monthly scale from 2005 to 2007 for each station. We acknowledge some uncertainty associated with the quality of the NCEP reanalysis data on the TP. Quantifying the moisture origins rigorously would require either a mass balance model driven by reanalyses or model outputs (e.g. Eltahir and Bras, 1994) or a water tagging approach (e.g. Koster et al., 1986), approaches having their own caveats (Gimeno et al., 2012). Here, for simplicity, we assume that back trajectories give an indication about the moisture origin. We chose to classify the monthly-clustered back trajectories at Lhasa and Nyalam into three categories (Fig. 5). The first category consists of moisture originating from the Mediterranean Sea, the Red Sea and the Atlantic Ocean. Moisture along these trajectories is transported eastward by the westerlies across Europe and central Asia

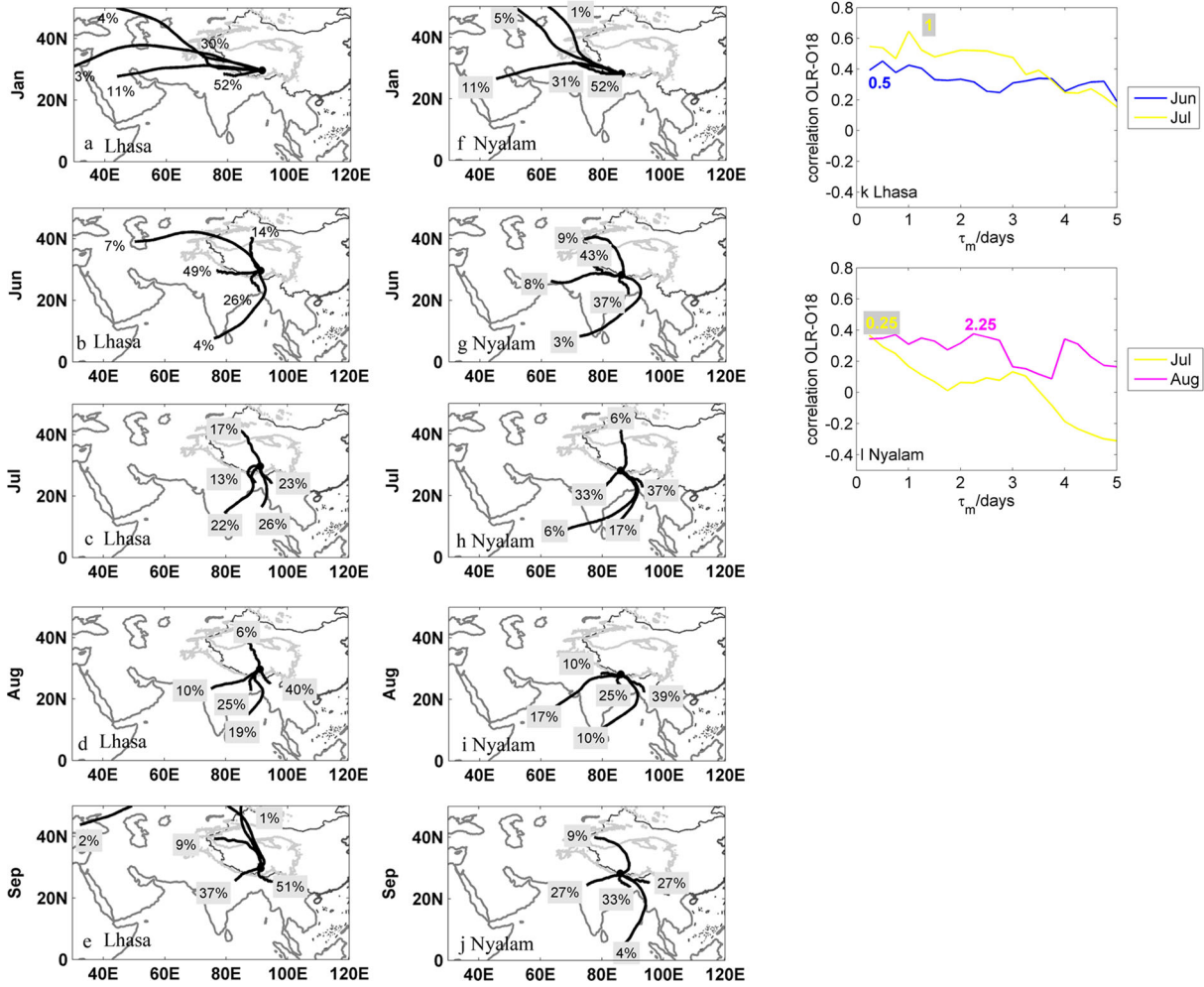


Fig. 5. (a–j) Back trajectories simulated by HYSPLIT for Lhasa and Nyalam in different months (January, June, July, August and September). The percentage shows the frequency of each clustered back trajectory. Correlation coefficient (R) between the precipitation $\delta^{18}\text{O}$ and OLR along the back trajectory averaged over J_m days (period prior to the event over which the convective activity is averaged) at Lhasa (k) and Nyalam (l). The numbers indicate the maximum values of J_m days for each period.

to the southern TP. The second category consists of continental trajectories, transporting moisture from various directions on short pathways. The third category consists of trajectories following the monsoon flow from the BOB and the AS. Moisture originating from the BOB moves along the Brahmaputra to the southern and interior TP (Tian et al., 2001; Gao et al., 2011); the other pathway from AS crosses the Indian peninsula and is then uplifted on the southern Himalayas. These pathways bring intense precipitation, resulting in heavily depleted ^{18}O in subsequent precipitation.

The different patterns of $\delta^{18}\text{O}$ at Nyalam and Lhasa may reflect different contributions of these three sources of moisture through time. In January, southern TP mostly receives moisture transported by the westerlies together with 50% of local sources (Fig. 5a and 5f). At Nyalam, this local moisture is transported along half shorter pathways than at Lhasa. This feature may account for enriched $\delta^{18}\text{O}$ in winter events at Nyalam. In JJA, moisture transport is dominated at Lhasa and Nyalam by advection from the BOB, which accounts for 30%–74% of trajectories (Fig. 5b, 5c, 5d, 5g, 5h and 5i). The second pathway to both stations is provided by the AS and above India, consistent with previous results (Feng and Zhou, 2012). A larger percentage of this second trajectory and transport paths above India is depicted for Nyalam compared to Lhasa in July (Fig. 5c and 5h). In September, moisture transport from the BOB still influences Nyalam, while it is weak at Lhasa (Fig. 5e and 5j).

Several events with more than 20 mm precipitation occur in non-monsoon seasons (e.g. events on 22 October 2005 and 24 September 2007) at Nyalam and Lhasa. The precipitation $\delta^{18}\text{O}$ values of those events are about 20% lower than that of events that occur in monsoon season. We find that, for these events, moisture is advected from the BOB (not shown). At Nyalam, these events are characterised by a significant negative correlation between precipitation amount and precipitation $\delta^{18}\text{O}$ ($R = -0.51$, $p < 0.05$), with no link with local OLR. The large depletion of these $\delta^{18}\text{O}$ events in the non-monsoon season may be explained by the local amount effect or by mixing with other moisture sources provided by the westerlies (Feng and Zhou, 2012). The moisture from BOB therefore also affects precipitation $\delta^{18}\text{O}$ in non-monsoon season. This suggests that, on longer time scales, slight changes in the advection of moisture from BOB may have very large impacts on precipitation weighted annual mean $\delta^{18}\text{O}$.

To detect the influence of convection along the back trajectories on precipitation $\delta^{18}\text{O}$ at Lhasa and Nyalam, we calculated the correlation coefficient between precipitation $\delta^{18}\text{O}$ and daily OLR along each trajectory over J_m days preceding the event (Fig. 5k and 5l). Because the correlation is valid only if air masses overflow the calculated sites, the

results during June and July at Lhasa and during July and August at Nyalam are discussed. At Lhasa, the precipitation $\delta^{18}\text{O}$ shows positive correlation with averaged OLR in June and July for days shorter than one day, while similar conditions are found at Nyalam in July and August. The shorter J_m days indicate the fast process of the moisture transport, and highlight the signature of integrated regional convective activity during the monsoon mature stage.

In this section, we show two dominant moisture transport paths during the monsoon season, one from the BOB and another one from the AS, which undergoes intense convection above northern India. This is very likely the reason why the convective activity westwards of our stations (“Zone 1”) plays a crucial role on southern TP $\delta^{18}\text{O}$.

3.4. Model-data comparison: illustration using the LMDZiso simulations

Atmospheric models equipped with water stable isotopes provide a comprehensive framework to investigate the relationships between precipitation isotopic composition and meteorological processes. Here, we use the LMDZiso model which has good global performance (Risi et al., 2010b) and performs reasonably well in the northern TP (Gao et al., 2011). The zoomed simulations overlap the 2005–2007 observation periods.

Some seasonal features of Lhasa precipitation $\delta^{18}\text{O}$ are present in our simulation. Although the model underestimates spring temperature and overestimates annual precipitation amount at Lhasa (Fig. 6a and 6b), it produces realistic variations of precipitation $\delta^{18}\text{O}$ (Fig. 6c). The model however seriously underestimates the frequency of the events with precipitation amounts above 10 mm and simulates too many events with low precipitation amount at Lhasa (Fig. 6g). At Nyalam, the model is not able to resolve several aspects of precipitation $\delta^{18}\text{O}$ variability (Fig. 6f). This may be related to artefacts in the seasonality of precipitation, as LMDZiso underestimates temperature but overestimates summer rainfall (Fig. 6d and 6e). The subseasonal distribution of precipitation events is therefore not in agreement with observations. At Nyalam, the model remarkably overestimates the frequency of the events with precipitation amounts above 10 mm (Fig. 6h). This may partly explain the unrealistic simulation of $\delta^{18}\text{O}$ at Nyalam. The model performance is representative of other models of this type (Gao et al., 2011). For Lhasa, LMDZiso underestimates the negative correlation between daily $\delta^{18}\text{O}$ and precipitation amount, compared with observations. The model-data comparison gives opposite results for Nyalam (not shown).

The influences of temperature or precipitation amount are explored in LMDZiso simulations using temporal

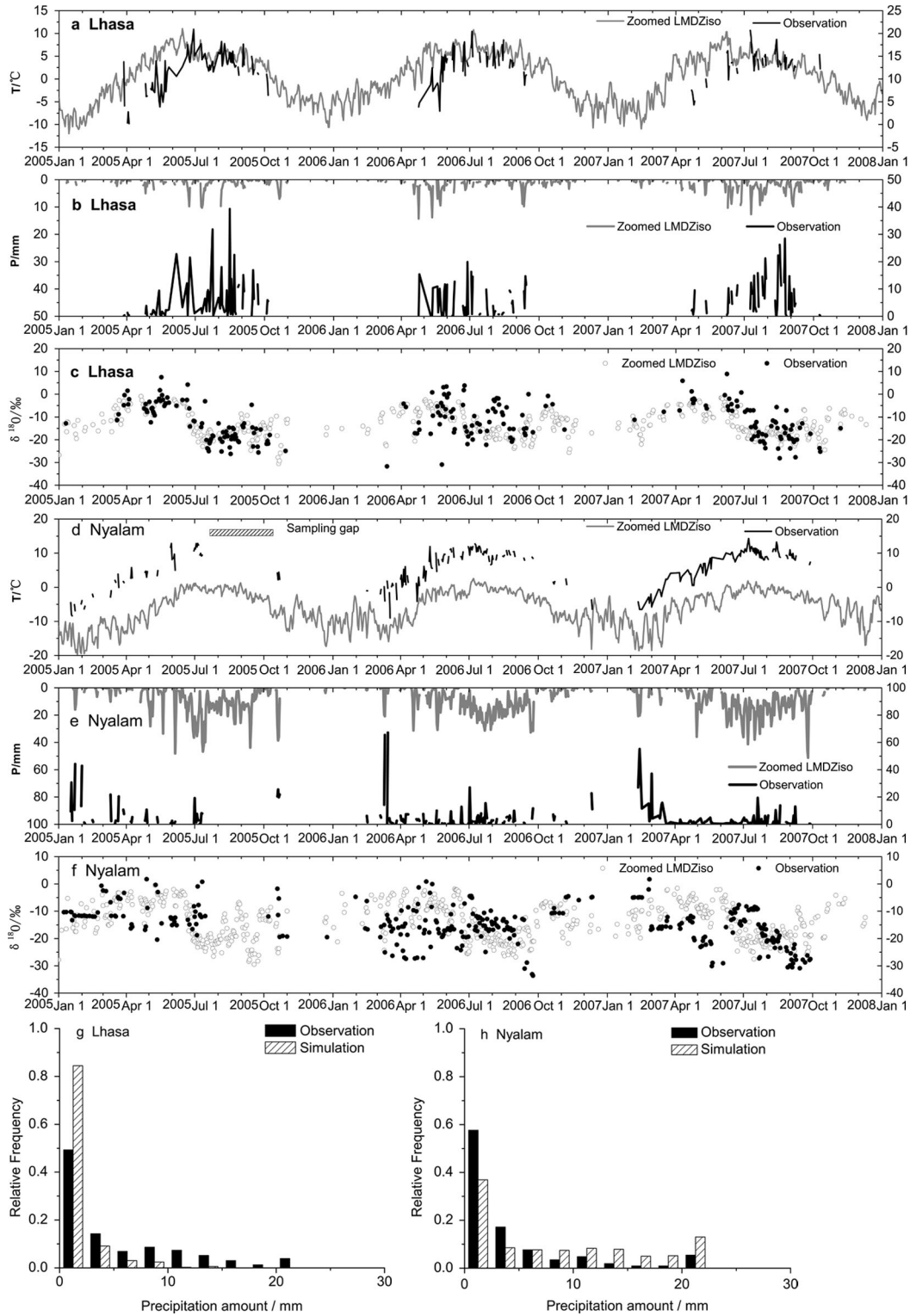


Fig. 6. Comparison of daily temperature from the zoomed LMDZiso simulations and observations at Lhasa (a) and Nyalam (d) during the observed period of 2005–2007; (b) and (e) same as (a) and (d) for precipitation amount; (c) and (f) same as (a) and (d) for precipitation $\delta^{18}\text{O}$. Relationships between precipitation amount and precipitation frequency at Lhasa (g) and Nyalam (h) from observations and zoomed LMDZiso simulations. The precipitation categories are calculated with steps of 2.5 mm, with events above 20 mm classified in one category.

correlations between daily $\delta^{18}\text{O}$ and temperature or precipitation amount. In summer, a clear positive correlation between daily $\delta^{18}\text{O}$ and local temperature is simulated for both Lhasa and Nyalam ($R=0.53$ and 0.40 , respectively, Fig. 7a and 7c), stronger than observed, while no correlation with local temperature is depicted in winter for both stations (Fig. 7b and 7d). In JJAS, LMDZiso simulates the weak negative correlation (R is ~ -0.2) between Lhasa precipitation $\delta^{18}\text{O}$ and precipitation amount in Zone 1 and south of Lhasa (Fig. 7e), stronger than derived from daily observation. For Nyalam in JJAS, LMDZiso simulates a strong negative correlation between $\delta^{18}\text{O}$ and precipitation in Zone 1 and north of the BOB (15°N – $25^\circ\text{N}/85^\circ\text{E}$ – 95°E , hereafter Zone 2, Fig. 7g). In DJF, LMDZiso simulates no significant correlation between precipitation $\delta^{18}\text{O}$ at Lhasa and precipitation amount (Fig. 7f), in agreement with the observation. However, stronger negative correlations are simulated with precipitation amount in north of Nyalam (Fig. 7h), opposite to observations. The stronger correlations between JJAS precipitation $\delta^{18}\text{O}$ and upstream precipitation simulated by LMDZiso compared to the data are consistent with previous studies in the West African and South American regions (Risi et al., 2010a; Vimeux et al., 2011). In these previous studies, it had been suspected that in LMDZiso, convection affects precipitation $\delta^{18}\text{O}$ over a downstream region that is not large enough. The patch of negative correlation simulated south of Lhasa and Nyalam

could be due to the fact that LMDZiso strongly overestimates convection in the BOB: LMDZiso overestimates precipitation by 30% in Zone 2. Therefore, it is expected that the effect of convection on precipitation $\delta^{18}\text{O}$ in this region is overestimated. The mismatch at Nyalam in DJF is also consistent with the overestimated precipitation in this region. To summarise, the reasonable agreement between the seasonal variations of precipitation $\delta^{18}\text{O}$ simulated by LMDZiso and observation in the southern TP therefore hides significant discrepancies in the way $\delta^{18}\text{O}$ responds to regional convective activity at the process scale. This calls for caution when using isotopic GCMs to investigate the links between archived $\delta^{18}\text{O}$ and past precipitation variability (Legrande and Schmidt, 2009; Pausata et al., 2011). Before undertaking such an investigation at paleo-time scales, it would be reasonable to check that the model is able to correctly simulate the links between $\delta^{18}\text{O}$ and convection at the intra-seasonal and seasonal scale. Our data provides a benchmark to evaluate this link. If this link is not properly represented, it casts some doubt on the model's capacity to properly represent this link at paleo-time scales.

4. Conclusions and perspectives

Taking advantage of several years of event precipitation sampling at two southern TP stations, we have investigated

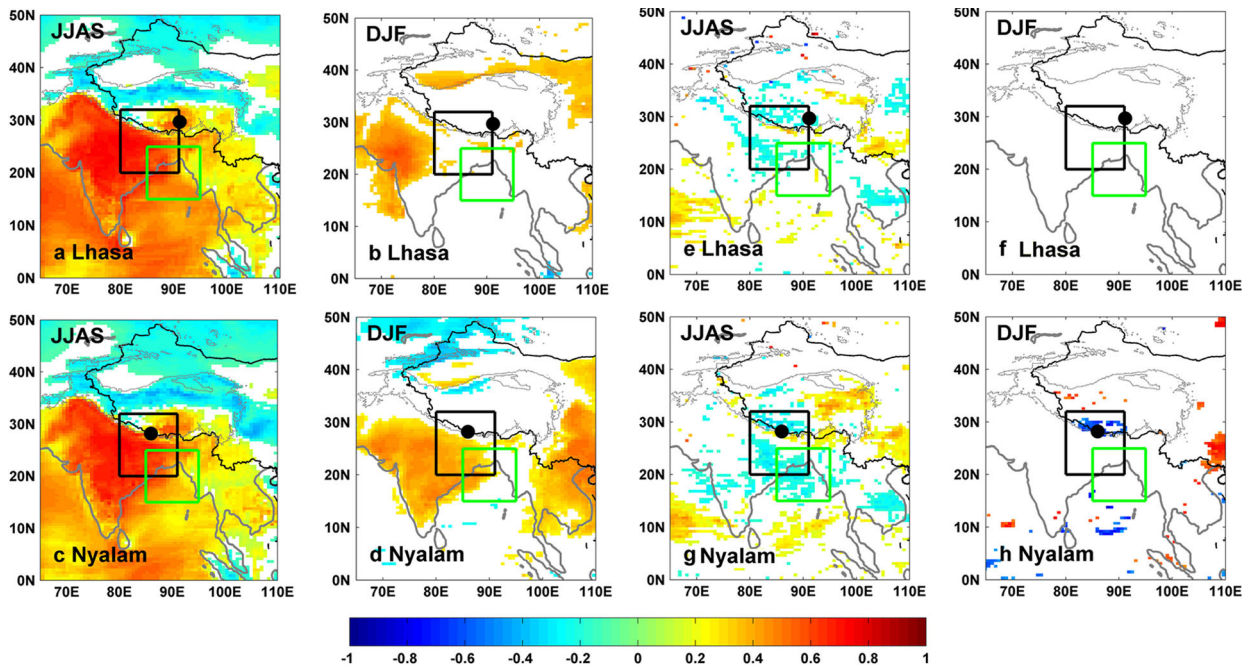


Fig. 7. Temporal correlation between temperature and precipitation $\delta^{18}\text{O}$ at Lhasa (a) and Nyalam (c) from zoomed LMDZiso simulations in summer (JJAS); (b) and (d) same as (a) and (c) for winter (DJF); (e) and (g) same as (a) and (c) for precipitation amount; (f) and (h) same as (e) and (g) for winter (DJF). The black rectangle shows the Zone 1, and the green rectangle shows the Zone 2.

the meteorological drivers of precipitation $\delta^{18}\text{O}$ at seasonal and intra-seasonal scales. Our results depict temperature effects at the event scale, even in summer. While a local amount effect is only evident for Lhasa at the event scale, local precipitation only accounts for a small fraction of $\delta^{18}\text{O}$ variability. At event and seasonal scales, convective activity is a main factor influencing precipitation $\delta^{18}\text{O}$ at Lhasa during the monsoon season, while it is the main driver at Nyalam only in July and August. Convective activity integrated over several days can explain less than 50% of the precipitation isotopic variance at both stations. Changes in the length of integration time are depicted to occur before, during and after the monsoon season, with large differences between Lhasa and Nyalam. The differences between the two stations may arise from different air mass trajectories, and the blocking effect of the high Himalayas. We conclude that precipitation $\delta^{18}\text{O}$ does not only reflect local climatic conditions, but also integrates regional upstream convective activity and precipitation. The correlation between cumulative convective activity and precipitation $\delta^{18}\text{O}$ is observed to be at a maximum when integrating over different periods, up to 20 d. Our results are consistent with recent findings from African and South American monsoon regions which also evidenced the importance of regional convective activity and upstream rainout (Vimeux et al., 2005; Vuille and Werner, 2005; Risi et al., 2008b). Considering studies on the relationship between Sea Surface Temperature (SST) and OLR (Srivastava et al., 2002; Krishnamurthy and Kirtman, 2009), we speculate that a relationship between SST and precipitation $\delta^{18}\text{O}$ may exist in the southern TP at the inter-annual time scale. Longer-term $\delta^{18}\text{O}$ observations are needed to investigate such relationships.

We have also evaluated the relationships between daily isotopic variability and regional climate in simulations conducted with one AGCM, LMDZiso, run in a nudged and zoomed configuration. While the model is able to produce seasonal characteristics of precipitation $\delta^{18}\text{O}$ at Lhasa, it overestimates the correlation with local meteorological variables and fails to capture the correlation between $\delta^{18}\text{O}$ and upstream convection (especially in Zone 1 and Zone 2). We show that the ability of a model to capture the seasonal patterns of precipitation $\delta^{18}\text{O}$ does not warrant that it correctly resolves the processes at play at the daily scale. This is particularly important when such models are used to assess the climatic controls of Asian $\delta^{18}\text{O}$ over longer time scales (LeGrande and Schmidt, 2009; Pausata et al., 2011). Further investigations are needed to assess the reason for the model-data mismatch. This may be due to dynamical processes (e.g. blocking of air masses by the Himalayas) and/or to physical processes (e.g. convection).

This model-data mismatch calls for a better documentation of the spatial and temporal variability of precipita-

tion isotopic composition ($\delta^{18}\text{O}$ but also second order parameters such as deuterium excess or ^{17}O -excess) in the southern TP and along air mass trajectories. Further investigations are needed to document the regional differences, especially with the focus of providing information relevant for the interpretation of high elevation ice core data.

Our results call for a very cautious interpretation of past variations of precipitation $\delta^{18}\text{O}$ such as archived indirectly in tree rings, speleothems, lake sediments or directly in glacier ice. The importance of upstream, integrated convection provides an explanation for the spatial heterogeneity between different records of the same archives (tree rings, Shi et al., 2011; ice cores, Zhao et al., 2011) within southern TP where the complex topographic situation likely favours site-specific moisture transport paths. Differences between different archives may further arise from different archiving processes and sampling of sub-seasonal precipitation for instance due to infiltration or tree growth seasonality. Our study is also consistent with the small correlation between southern TP ice core $\delta^{18}\text{O}$ and accumulation variations. While we demonstrate the lack of simple relationships between precipitation $\delta^{18}\text{O}$ and local climate parameters, we also show that archives of precipitation $\delta^{18}\text{O}$ have the potential to offer integrated information on regional convective activity related with moisture transport paths. Investigations of the mechanisms controlling precipitation $\delta^{18}\text{O}$ at the inter-annual to decadal scale are required prior to precise interpretations. Our findings suggest that a matrix of spatial and temporal past precipitation $\delta^{18}\text{O}$ variations from coastal areas to southern TP could allow tracking past changes in moisture fluxes.

5. Acknowledgements

This work was funded by the National Natural Science Foundation of China (Grants 41101061 and 41190080), the ‘Strategic Priority Research Program (B)’ of the Chinese Academy of Sciences, Grant No. XDB03030100, the Caiyuanpai Programme and the open research foundation of State Key Laboratory of Cryospheric Sciences, Cold and Arid Regions Environment and Engineering Research Institute, CAS. We also thank the staff at Tibet observation stations for collecting the precipitation samples and for taking simultaneous notes, and the staff for measuring the samples.

References

- Aggarwal, P. K., Alduchov, O. A., Froehlich, K. O., Araguas-Araguas, L. J., Sturchio, N.C. and co-authors. 2012. Stable isotopes in global precipitation: a unified interpretation based on atmospheric moisture residence time. *Geophys. Res. Lett.* **39**, L11705. DOI: 10.1029/2012GL05193.

- Aggarwal, P. K., Fröhlich, K., Kulkarni, K. M. and Laurence, L. 2004. Stable isotope evidence for moisture sources in the Asian summer monsoon under present and past climate regimes. *Geophys. Res. Lett.* **31**, L08203. DOI: 10.1029/2004GL019911.
- Aizen, V. B., Aizen, E. M., Joswiak, D. R., Fujita, K., Takkeuchi, N. and co-authors. 2006. Climatic and atmospheric circulation pattern variability from ice-core isotope/geochemistry records (Altai, Tien Shan and Tibet). *Ann. Glaciol.* **43**, 49–60.
- An, W., Liu, X., Leavitt, S. W., Ren, J., Sun, W. and co-authors. 2012. Specific climatic signals recorded in earlywood and latewood $\delta^{18}\text{O}$ of tree rings in southwestern China. *Tellus B.* **64**, 18703.
- An, Z., Clemens, S. C., Shen, J., Qiang, X., Jin, Z. and co-authors. 2011. Glacial–interglacial Indian summer monsoon dynamics. *Science*. **333**(6043), 719–723.
- Araguas-Araguas, L., Froehlich, K. and Rozanski, K. 1998. Stable isotope composition of precipitation over southeast Asia. *J. Geophys. Res. Atmos.* **103**, 28721–28742.
- Bony, S., Risi, C. and Vimeux, F. 2008. Influence of convective processes on the isotopic composition ($\delta\text{O}-18$ and δD) of precipitation and water vapor in the tropics: 1. Radiative–convective equilibrium and Tropical Ocean–Global Atmosphere–Coupled Ocean–Atmosphere Response Experiment (TOGA–COARE) simulations. *J. Geophys. Res. Atmos.* **113**, D19305, 148–227.
- Cai, Y., Cheng, H., An, Z., Edwards, R. L. and co-authors. 2010. Large variations of oxygen isotopes in precipitation over south-central Tibet during Marine Isotope Stage 5. *Geology*. **38**(3), 243–246.
- Chakravarty, K., Raj, P. E., Bhattachaiya, A. and Maitra, A. 2013. Microphysical characteristics of clouds and precipitation during pre-monsoon and monsoon period over a tropical Indian station. *J. Atmos. Sol. Terr. Phys.* **94**, 28–33.
- Danis, P. A., Masson-Delmotte, V., Stievenard, M., Guillemin, M. T., Daux, V. and co-authors. 2006. Reconstruction of past precipitation $\delta^{18}\text{O}$ using tree-ring cellulose $\delta^{18}\text{O}$ and $\delta^{13}\text{C}$: a calibration study near Lac d’Annecy, France. *Earth Planet. Sci. Lett.* **243**(3–4), 439–448.
- Dansgaard, W. 1964. Stable isotopes in precipitation. *Tellus*. **16**(4), 436–468.
- DeCelles, P. G., Quade, J., Kapp, P., Fan, M., Dettman, D. L. and Ding, L. 2007. High and dry in central Tibet during the Late Oligocene. *Earth Planet. Sci. Lett.* **253**(3–4), 389–401.
- Eltahir, E. A. B. and Bras, R. L. 1994. Precipitation recycling in the Amazon basin. *Q. J. R. Meteorol. Soc.* **120**(518), 861880. DOI: 10.1002/qj.49712051806.
- Feng, L. and Zhou, T. 2012. Water vapor transport for summer precipitation over the Tibetan Plateau: multidata set analysis. *J. Geophys. Res.* **117**, D20114. DOI: 10.1029/2011JD017012.
- Gao, J., Masson-Delmotte, V., Yao, T., Tian, L., Risi, C. and co-authors. 2011. Precipitation water stable isotopes in the South Tibetan Plateau: observations and modeling. *J. Clim.* **24**, 3161–3178.
- Gimeno, L., Stohl, A., Trigo, R. M., Dominguez, F., Yoshimura, K. and co-authors. 2012. Oceanic and terrestrial sources of continental precipitation. *Rev. Geophys.* **50**, RG4003. DOI: 10.1029/2012RG000389.
- Grießinger, J., Bräuning, A., Helle, G., Thomas, A. and Schleser, G. 2011. Late Holocene Asian summer monsoon variability reflected by $\delta^{18}\text{O}$ in tree-rings from Tibetan junipers. *Geophys. Res. Lett.* **38**(L03), L03701.
- Henderson, A. C. G., Holmes, J. A. and Leng, M. J. 2010. Late Holocene isotope hydrology of Lake Qinghai, NE Tibetan Plateau: effective moisture variability and atmospheric circulation changes. *Quaternary Sci. Rev.* **29**(17–18), 2215–2223.
- Hoffmann, G. and Heimann, M. 1997. Water isotope modeling in the Asian monsoon region. *Quat. Int.* **37**, 115–128.
- Ishizaki, Y., Yoshimura, K., Kanae, S., Kimoto, M., Kurita, N. and co-authors. 2012. Interannual variability of $\text{H}_2\ ^{18}\text{O}$ in precipitation over the Asian monsoon region. *J. Geophys. Res.* **117**, D16307. DOI: 10.1029/2011JD015890.
- Johnson, K. R. and Ingram, B. L. 2004. Spatial and temporal variability in the stable isotope systematics of modern precipitation in China: implications for paleoclimate reconstructions. *Earth Planet. Sci. Lett.* **220**, 365–377.
- Joswiak, D. R., Yao, T., Wu, G., Xu, B. and Zheng, W. 2010. A 70-yr record of oxygen-18 variability in an ice core from the Tanggula Mountains, central Tibetan Plateau. *Clim. Past*. **6**, 219–227.
- Kaspari, S., Mayewski, P., Kang, S., Sneed, S., Hou, S. and co-authors. 2007. Reduction in northward incursions of the South Asian monsoon since ~1400 AD inferred from a Mt. Everest ice core. *Geophys. Res. Lett.* **34**, 16, 94–8276.
- Kong, Y., Pang, Z. and Froehlich, K. 2013. Quantifying recycled moisture fraction in precipitation of an arid region using deuterium excess. *Tellus B.* **65**, 19251.
- Koster, R., Jouzel, J., Suozzo, R., Russell, G., Broecker, W. and co-authors. 1986. Global sources of local precipitation as determined by the NASA/GISS GCM. *Geophys. Res. Lett.* **13**(2), 121124. DOI: 10.1029/GL013i002p00121.
- Krishnamurthy, V. and Kirtman, P. B. 2009. Relation between Indian Monsoon Variability and SST. *J. Clim.* **22**, 4437–4458.
- Lee, J.-E., Pierrehumbert, R., Swann, A. and Lintner, B. R. 2009. Sensitivity of stable water isotopic values to convective parameterization schemes. *Geophys. Res. Lett.* **36**, L23801. DOI: 10.1029/2009GL040880.
- LeGrande, A. N. and Schmidt, G. A. 2009. Sources of holocene variability of oxygen isotopes in paleoclimate archives. *Clim. Past*. **5**(3), 441–455.
- Lewis, S. C., LeGrande, A. N., Kelley, M. and Schmidt, G. A. 2010. Water vapour source impacts on oxygen isotope variability in tropical precipitation during Heinrich events. *Clim. Past*. **6**, 325–343.
- Pausata, F., Battisti, D. S., Nisancioglu, K. H. and Bitz, C. M. 2011. Chinese stalagmite $\delta^{18}\text{O}$ controlled by changes in the Indian monsoon during a simulated Heinrich event. *Nat. Geosci.* **4**(7), 474–480.
- Risi, C., Bony, S. and Vimeux, F. 2008a. Influence of convective processes on the isotopic composition ($\delta^{18}\text{O}$ and δD) of precipitation and water vapor in the tropics: 2. Physical interpretation of the amount effect. *J. Geophys. Res. Atmos.* **113**, D19, 148–227.
- Risi, C., Bony, S., Vimeux, F., Descroix, L., Ibrahim, B. and co-authors. 2008b. What controls the isotopic composition of

- the African monsoon precipitation? Insights from event-based precipitation collected during the 2006 AMMA field campaign. *Geophys. Res. Lett.* **35**, L24808.
- Risi, C., Bony, S., Vimeux, F., Frankenberg, C. and Noone, D. 2010a. Understanding the Sahelian water budget through the isotopic composition of water vapor and precipitation. *J. Geophys. Res.* **115**, D24110. DOI: 10.1029/2010JD014690.
- Risi, C., Bony, S., Vimeux, F., Jouzel, J., Masson-Delmotte, V. and co-authors. 2010b. Water stable isotopes in the LMDZ4 general circulation model: model evaluation for present day and past climates and applications to climatic interpretations of tropical isotopic records. *J. Geophys. Res.* **115**, D12118. DOI: 10.1029/2009JD013255.
- Shi, C., Masson-Delmotte, V., Risi, C., Eglin, T., Stievenard, M. and co-authors. 2011. Sampling strategy and climatic implications of tree-ring stable isotopes on the southeast Tibetan Plateau. *Earth Planet. Sci. Lett.* **301**(1–2), 307–316.
- Srivastava, A. K., Rajeevan, M. and Kulkarni, R. 2002. Teleconnection of OLR and SST anomalies over Atlantic Ocean with Indian summer monsoon. *Geophys. Res. Lett.* **29**(8), 1284. DOI: 10.1029/2001GL013837.
- Thompson, L. G., Yao, T., Davis, M. E., Henderson, K. A., Mosley-Thompson, E. and co-authors. 1997. Tropical climate instability: the last glacial cycle from a Qinghai-Tibetan Ice Core. *Science*. **276**(5320), 1821–1825.
- Thompson, L.G., Yao, T., Mosley-Thompson, E., Davis, M. E., Henderson, K. A. and co-authors. 2000. A high-resolution millennial record of the South Asian Monsoon from Himalayan Ice Cores. *Science*. **289**, 1916–1919.
- Tian, L., Masson-Delmotte, V., Stievenard, M., Yao, T. and Jouzel, J. 2001. Tibetan Plateau summer monsoon northward extent revealed by measurements of water stable isotopes. *J. Geophys. Res.* **106**, 28081–28088.
- Tian, L., Yao, T., Schuster, P. F., White, J. W. C., Ichiyani, K. and co-authors. 2003. Oxygen-18 concentrations in recent precipitation and ice cores on the Tibetan Plateau. *J. Geophys. Res. Atmos.* **108**, D9, 161–169.
- Tremoy, G., Vimeux, F., Mayaki, S., Souley, I., Cattani, O. and co-authors. 2012. A 1-year long $\delta^{18}\text{O}$ record of water vapor in Niamey (Niger) reveals insightful atmospheric processes at different timescales. *Geophys. Res. Lett.* **39**, L08805. DOI: 10.1029/2012GL051298.
- Tyrlis, E., Lelieveld, J. and Steil, B. 2013. The summer circulation over the eastern Mediterranean and the Middle East: influence of the South Asian monsoon. *Clim. Dynam.* **40**, 1103–1123.
- Van Leer, B. 1977. Towards ultimate conservative difference scheme: IV. A new approach to numerical convection. *J. Comput. Phys.* **23**, 276–299.
- Vimeux, F., Gallaire, R., Bony, S., Hoffmann, G. and Chiang, J. C. H. 2005. What are the climate controls on (D) in precipitation in the Zongo Valley (Bolivia)? Implications for the Illimani ice core interpretation. *Earth Planet. Sci. Lett.* **240**, 205–220.
- Vimeux, F., Tremoy, G., Risi, C. and Gallaire, R. 2011. A strong control of the South American SeeSaw on the intra-seasonal variability of the isotopic composition of precipitation in the Bolivian Andes. *Earth Planet. Sci. Lett.* **307**, 47–58.
- Vuille, M. and Werner, M. 2005. Stable isotopes in precipitation recording South American summer monsoon and ENSO variability: observations and model results. *Clim. Dynam.* **25**(4), 401–413. DOI: 10.1007/s00382-005-0049-9.
- Vuille, M., Werner, M., Bradley, R. S. and Keimig, F. 2005. Stable isotopes in precipitation in the Asian monsoon region. *J. Geophys. Res.* **110**(D23), D23108.
- Wang, B. and Xu, X. 1997. Northern Hemisphere summer monsoon singularities and climatological intraseasonal oscillation. *J. Clim.* **10**, 1171–1185.
- Wang, N., Yao, T., Pu, J., Zhang, Y., Sun, W. and Wang, Y. 2003. Variations in air temperature during the last 100 years revealed by (18O) in the Malan ice core from Tibetan Plateau. *Chin. Sci. Bull.* **48**, 2134–2138.
- Wang, Y., Cheng, H., Edwards, R. L., He, Y., Kong, X. and co-authors. 2005. The Holocene Asian monsoon: links to solar changes and North Atlantic climate. *Science*. **308**, 854–857.
- Wu, G., Guan, Y., Liu, Y., Yan, J. and Mao, J. 2012. Air-sea interaction and formation of the Asian summer monsoon onset vortex over the Bay of Bengal. *Clim. Dynam.* **38**, 261–279.
- Yao, T., Guo, X., Thompson, L.G., Duan, K., Wang, N. and co-authors. 2006. $\delta^{18}\text{O}$ record and temperature change over the past 100 years in ice cores on the Tibetan Plateau. *Sci. China (D)* **49**, 1–9.
- Yao, T., Thompson, L.G., Mosley-Thompson, E. and Yang, Z. 1996. Climatological significance of $\delta^{18}\text{O}$ in north Tibetan ice cores. *J. Geophys. Res.* **101**(D23), 29531–29537.
- Yao, T., Thompson, L., Yang, W., Yu, W., Gao, Y. and co-authors. 2012. Different glacier status with atmospheric circulations in Tibetan Plateau and surroundings. *Nat. Clim. Change*. **2**, 663–667. DOI: 10.1038/NCLIMATE1580.
- Zhang, D., Qin, D., Hou, S., Kang, S., Ren, J. and co-authors. 2005. Climate significance of (18O) records from an 80.36 m ice core in the East Rongbuk Glacier, Mount Qomolangma (Everest). *Sci. China (D) Earth Sciences*. **48**(2), 266–272.
- Zhao, H., Xu, B., Yao, T., Lin, S., Gao, J. and co-authors. 2011. Deuterium excess record in a southern Tibetan ice core and its potential climatic implications. *Clim. Dynam.* **38**, 1791–1803.